Microstructure and Mechanical Properties of Aluminum Clad Steel Plates by Cold Rolling and Annealing Heat Treatment

Fuxing Yin, Jiule Ma, Baoxi Liu, Jining He, Fanyong Zhang, Mingyang Liu and Yanchun Dong

Abstract Aluminum clad steel plate has been successfully fabricated by cold rolling and annealing heat treatment. The thicknesses of total clad plate and aluminum cladding layer were about 1.5 mm and 50–70 μm, respectively. The grain morphology, mechanical properties revealed a slight anisotropy. Herein, the grains were severe elongated along the cold rolling direction. The clad plates exhibited a superior tensile elongation and slight interfacial delamination, and highest value of multiple bending fracture times was located at the clad plate along the angle of 45°. Moreover, the perfect interfacial brazing bonding presented at the base clad plate and fins, which can be used in the power station.

Keywords Aluminum clad steel plate · Cold rolling and annealing
Elongated grain · Mechanical anisotropy · Interfacial delamination

F. Yin · B. Liu (✉) · J. He · F. Zhang · M. Liu · Y. Dong
School of Materials Science and Engineering, Research Institute for Energy Equipment Materials, TianJin Key Laboratory of Materials Laminating Fabrication and Interfacial Controlling Technology, Hebei University of Technology, Tianjin 300132, China
e-mail: liubaoxiliubo@126.com

F. Yin
e-mail: yinfuxing@hebut.edu.cn

J. He
e-mail: hbgdhjn@126.com

F. Zhang
e-mail: fany_zhang@163.com

M. Liu
e-mail: twzzyyx@126.com

Y. Dong
e-mail: hbgddych@163.com

J. Ma
School of Materials Science and Engineering, Hebei University of Science and Technology, Shijiazhuang 050080, China
e-mail: jdsrsjz@163.com

Y. Han (ed.), *Advances in Materials Processing*, Lecture Notes in Mechanical Engineering, https://doi.org/10.1007/978-981-13-0107-0_61

Introduction

Aluminum clad steel sheet has the advantages of high corrosion resistance, thermal conductivity of aluminum alloy and high mechanical properties of steel, which is the main base materials of the cooling tube bundle in the power station. The single row tube of air cooling system is composed of aluminum clad steel sheet, and the Al cladding can be easily brazed with Al aluminum fins to form a tube bundle element. A strong interfacial bonding strength can also obtained between clad sheet and Al fins, and the whole area of the heat exchange tube can be also involve in heat transfer [1–3].

However, there are big difference between aluminum and iron on the atom radius, melting point, density, linear thermal expansion coefficient, and lattice parameters etc. Meanwhile, Al taken as one of the most typical electronegative element can easily react with many positive electrical metallic elements and form brittle intermetallics. For example, many solid solutions, intermetallics ($FeAl_3$, $FeAl_2$, Fe_2Al_5, Fe_4Al_{13}) and eutectics are generated based on the reaction between Fe and Al elements, which seriously limit the fabrication and practical application of aluminum clad steel sheet [4–10].

There are many methods to fabricate aluminum clad steel sheet, such as solid-state bonding [11], accumulative roll bonding [12], warm rolling [13], friction stir welding [14, 15], Defocused Laser Beam [16], butt TIG welding [2], spot welding [17], explosive welding [18], hot rolling [19, 20], and cold rolling [21–24] etc. Herein, many interfacial reaction particles and oxides are easily formed during hot and warm rolling or welding processes, which seriously deteriorate interfacial bonding strength of aluminum clad steel sheet [2, 25].

Recently, the cold roll bonding is the most economic and effective fabrication process among these various technologies [3, 26]. However, there are many difficulties in cold roll bonding process on aluminum clad steel sheet. Firstly, asymmetric deformation in the roll-gap will result in different thickness reduction and wraping phenomena between the two individual sheets due to different flow stresses [27–29]. Secondly, the interfacial bonding strength and stable interface can be effectively affected by many process parameters, such as surface roughness, rolling load, rolling speed, first pass reduction in thickness, thickness ratio, and heat treatment parameters [3, 26, 30–34]. Thirdly, the mechanical properties of cold rolled aluminum clad steel sheet present a low formability due to anisotropy [35]. The aim of this study was to investigate anisotropy and welding behavior of aluminum clad steel sheet, and make a guide to understand the relationship between microstructure and performance.

Experimental Procedures

The compositions of commercial pure aluminum and commercial pure steel plates are shown in Table 1, were used as raw materials. Firstly, in order to obtain perfect bonding, it is necessary to remove contaminant layers present on the surface of the contacting plates, these layers are composed of oxides, adsorbed ions (ions of sulfur, phosphor and oxygen), grease, and humidity and dust particles. Therefore, negative pressure degreasing and wire brushing of two contacting surface of the Al/Fe sheets were carried out using a stainless steel circumferential brush operating at a rotation speed of 2500 rpm/min. Moreover, scratch brushing is not only for cleaning but also for providing rough surfaces, which provide a greater amount of surface asperities and promote a localized shear deformation that breaks unavoidable surface oxide films during cold roll bonding, contributing to the firm bonding of aluminum clad steel sheets. The initial thicknesses of Al and Fe were 0.25 mm and 4.0 mm, respectively. The cold roll bonding process was performed under lubricated condition by 50 and 75% in the first and final rolling pass. Li et al. [3] proposed that the interfacial bonding strength did not develop until reduction greatly exceeded the reduction (50%). The cold rolling mills with roll diameter of 550 mm possess 8 rollers and the rolling speed was 360 rpm/min. Finally, the cold-rolled aluminum clad steel sheets were annealed at 450 °C for 120 min as shown in Fig. 1a.

Figure 1b shows the three directions in the rolling plane (I plane): rolling direction, transverse direction and normal direction. The three perpendicularly planes are named as I, II and III plane, respectively. The uniaxial tensile tests on flat specimens were carried out in order to determine the mechanical properties. The samples were cut from aluminum clad steel sheet in five directions at mentioned angles: $\alpha = 0°$, 30°, 45°, 60°, 90° in relation to direction of cold rolling. The geometry of the bimetallic specimen is presented in Fig. 2. All tests of uniaxial tensile of specimens were performed on an universal testing machine Instron-5569 plus with traverse speed of 2 mm/min. Measurement of longitudinal deformation took place by using an extensometer of gauge length 10 mm. Starting load of specimen was 0.1 kN.

Table 1 Chemical compositions of the raw materials used in Al/Fe clad plates

Commercial pure Al								
Elements	Al	Si	Fe	Cu	Mn	Ni	Cr	C
wt%	98.71	0.85	0.41	0.01	0.01	0.01	–	–
Commercial pure Fe								
Elements	Fe	C	Si	Mn	P	S	Al	N
wt%	99.71	0.005	0.01	0.24	0.016	0.01	0.001	0.006

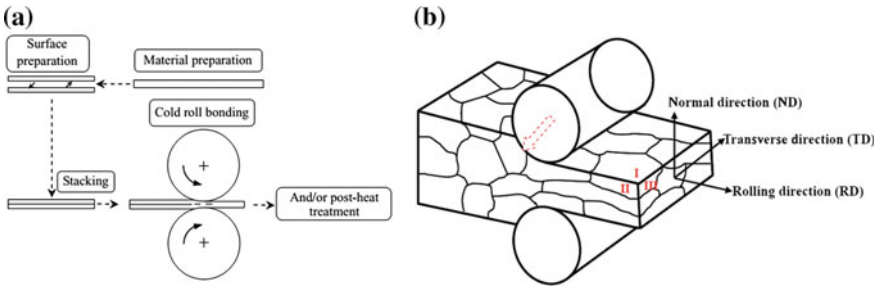

Fig. 1 Schematic illustration showing principle of cold roll bonding (CRB), **a** fabrication process; **b** microstructure evolution during the cold rolling

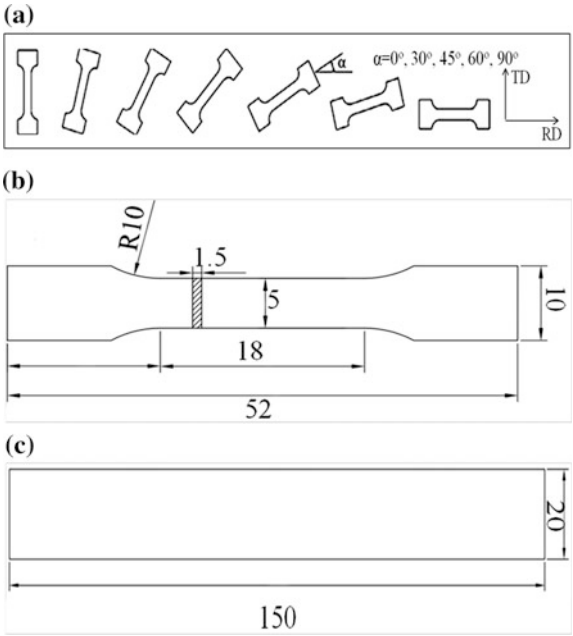

Fig. 2 Geometry of the bimetallic specimen, **a** scheme of cutting of tensile samples from I section; **b** tensile sample; **c** multiple bending sample

Microstructural examinations and fracture characterizations were performed using optical microscopy (OM) and scanning electron microscopy (SEM, Hitachi S-4700) on the aluminum clad steel sheet after etching using a 4% HNO_3 alcohol solution. In order to attain a clear surface, the specimens were glued to a metallic plate and polished using a polishing machine.

Results and Discussions

Figure 3 shows the optical microstructure of aluminum clad steel plate by cold rolling and annealing heat treatment. The total thickness of aluminum clad steel plate is about 1.5 mm, and the aluminum cladding layer is straight, uniform and continuous as shown in Fig. 3a. Herein, the thickness of aluminum cladding layer is about 50–70 μm, as shown in Fig. 3b, and many grains of steel substrate are elongated along the rolling direction [36]. The average size of transverse linear interception for the elongated grains was 10 μm. However, the grains of II cross section are uniform and equiaxed as shown in Fig. 3c, and average size is about 30 μm. Figure 3d shows the microstructure of III cross section, and the average size of equiaxed grain is about 60 μm, the unique grain characteristics of I, II and III cross sections are attributed to the high rolling reduction ratio [37]. The original 3D equiaxed grains are changed to one pancake-like microstructure due to its special deformation characteristics. The grain size is enlarged along the rolling surface, while the transverse linear interception for the elongated grains decreases with the increase of rolling reduction ratio [38].

Figure 4 shows the engineering and true stress-strain curves of aluminum clad steel plates along different angle, and Tables 2 and 3 list the corresponding values of tensile properties. The stress-strain curves reveal a similar elastic deformation and prolong uniform plastic deformation stages. Elastic properties of the tested

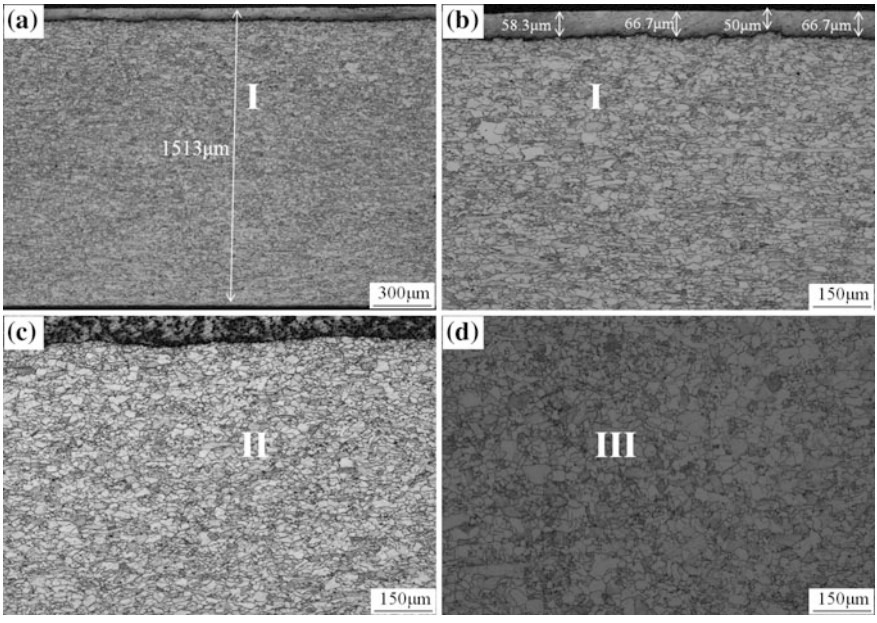

Fig. 3 Microstructure of aluminum clad steel plate. **a** Macroscopic picture; **b** the I cross section; **c** the II cross section; **d** the III cross section

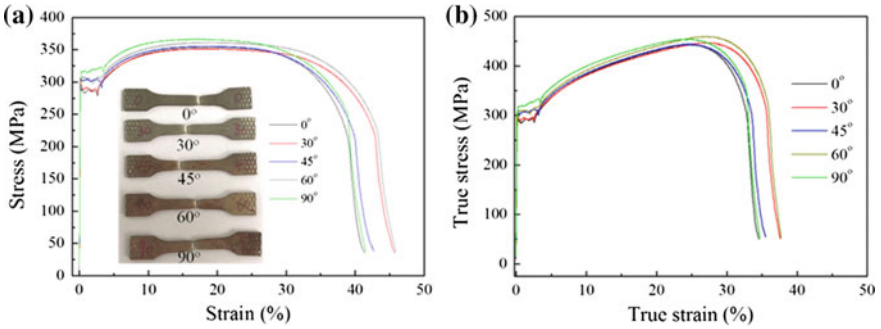

Fig. 4 Sstress-strain curves of aluminum clad steel plates with different angle. **a** Engineering stress-strain curves; **b** true stress-strain curves

Table 2 Mechanical properties of aluminum clad steel plates with different angles

Angle (°)	Elastic modulus (GPa)	Yielding strength (MPa)	Ultimate strength (MPa)	Elongation (%)
0	180	289	354	41.3
30	171	294	352	45.7
45	177	302	356	42.6
60	181	307	361	45.8
90	185	316	367	41.5

Table 3 Calculated mechanical parameters of aluminum clad steel plates with different angles

Angle (°)	K (MPa)	n	$\sigma_{necking}$ (MPa)
0	253	0.178	422
30	256	0.171	417
45	261	0.169	421
60	262	0.172	429
90	278	0.157	428

aluminum clad steel plates were represented by Young's modules E. The values of Young's modules (171 GPa) of clad plate were lowest in the direction $\beta = 30°$, and largest value (185 GPa) in the direction $\beta = 90°$. Relative differences between the extreme values of Young's modules were 8.18% for aluminum clad steel plate. It is observed that the values of yield strength ($\sigma_{0.2}$) and ultimate strength (σ_b) are gradually increased with the increasing tensile angle. The slight anisotropy of mechanical properties of the tested aluminum clad steel plates was undoubtedly the result of technological processes during the rolling process and subsequent annealing heat treatment. The cold rolling process and interfacial bonding of aluminum and steel layers in the clad plates need to use high rolling force, which generated the clad plate anisotropy. Meanwhile, the annealing heat treatment

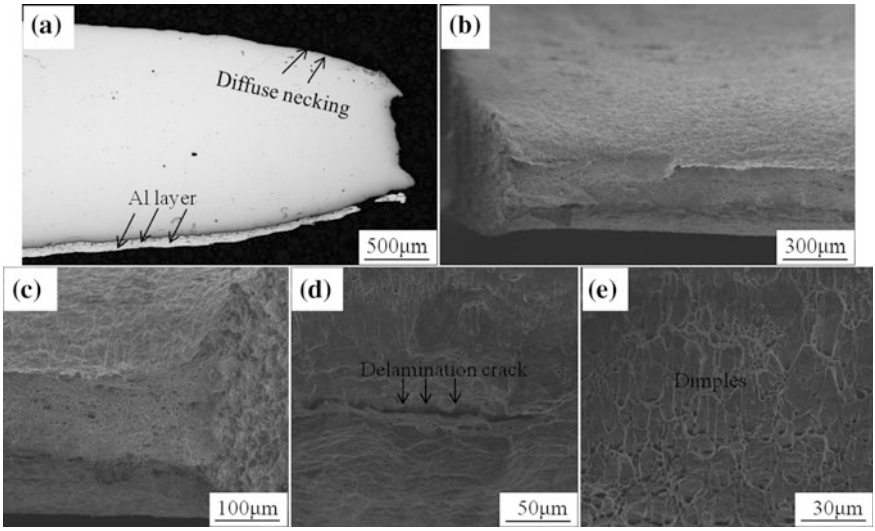

Fig. 5 Tensile fracture characteristics of aluminum clad steel plate. **a** Macroscopic picture; **b**, **c** microscopic pictures; **d** interfacial delamination; **e** steel substrate

eliminates the partial residual stress and severe mechanical anisotropy. Moreover, based on the power low equation as shown:

$$\sigma = K\,\varepsilon^{n} \tag{1}$$

where K and n are taken as strength coefficient and strain hardening exponent, respectively. The power low equation has been successfully used to predict the true stress-strain relation. The relation is obtained by fitting the true stress-strain relation calculated by Eq. (1) according to empirical data until the maximum load point. The values of K, n, critical strain ($\varepsilon_{necking}$) and critical stress ($\sigma_{necking}$) at the necking point are listed in Table 3. Herein, high value of n shows the prolonged uniform deformation capacity and high formability [39]. The lowest value of n is 0.157 along the cold rolling direction $\beta = 90°$, and the highest value of n is 0.178 along the cold rolling direction $\beta = 0°$. Relative differences between the extreme values of n were 13.36% for aluminum clad steel plate. Overall, the aluminum clad steel plates reveal a slight mechanical and formability anisotropy.

Figure 5 shows the tensile fracture characteristics of aluminum clad steel plate. The enlarged edge view of the fractured tensile sample reveals an uncontinuous aluminum cladding layer and thickness-wise necking morphologies as shown in Fig. 5a.

Meanwhile, a slight interfacial delamination crack is formed at the fracture position. The delamination along the interface was observed in the aluminum clad steel plate as shown in Fig. 5d. The interfacial crack developed slight open with strain and the debonded Al and Fe plate deformed separately. The weak interface is

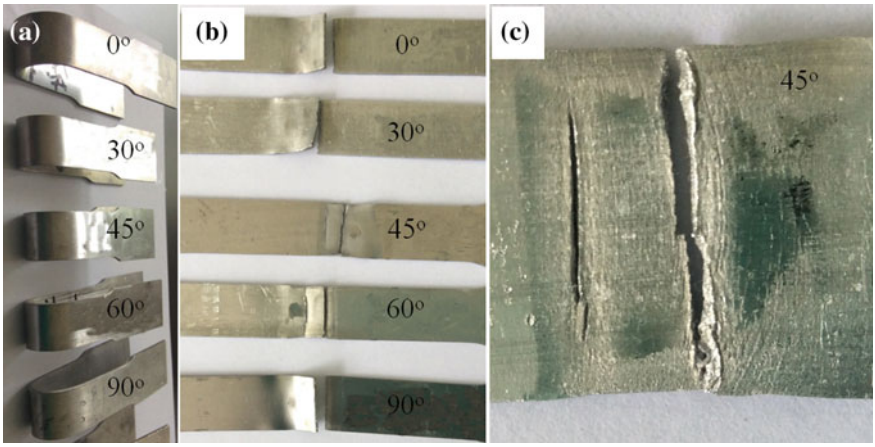

Fig. 6 Cold bending and multiple bending morphologies of aluminum clad steel plates. **a** Cold bending samples; **b** multiple bending fracture morphologies; **c** The microscopic fracture characteristics of multiple bending sample along the angle of 45°

attributed to the interfacial intermetallic layer. In addition, many refined dimples are presented in the steel substrate as shown in Fig. 5e, revealing a typical ductile fracture characteristic.

Figure 6 shows the cold bending and multiple bending morphologies of aluminum clad steel plates. There are no interfacial delamination and fracture characteristics found in the bending samples with different angles along cold rolling direction, exhibiting the perfect interfacial bonding between aluminum cladding and steel substrate as shown in Fig. 6a. Figure 6b shows the multiple bending fracture characteristics of aluminum clad steel plates, and the fold times are listed in the Table 4. It is revealed that the highest value (75 times) of fold times is located at the aluminum clad steel plate along the angle of 45°, and the lowest value (60 times) is present at the clad plate along the angle of 0°. Therefore, the aluminum clad steel plate along the angle of 45° exhibits a high formability. Figure 6c shows the microscopic fracture characteristics of aluminum clad steel plates. Beside the main crack, there is the second crack present at the clad plate, and there are no interfacial delamination phenomena, exhibiting a superior interfacial bonding quality.

Table 4 Fold times of multiple bending aluminum clad steel plates with different angles

Angle (°)	Fold times
0	55
30	66
45	75
60	64
90	60

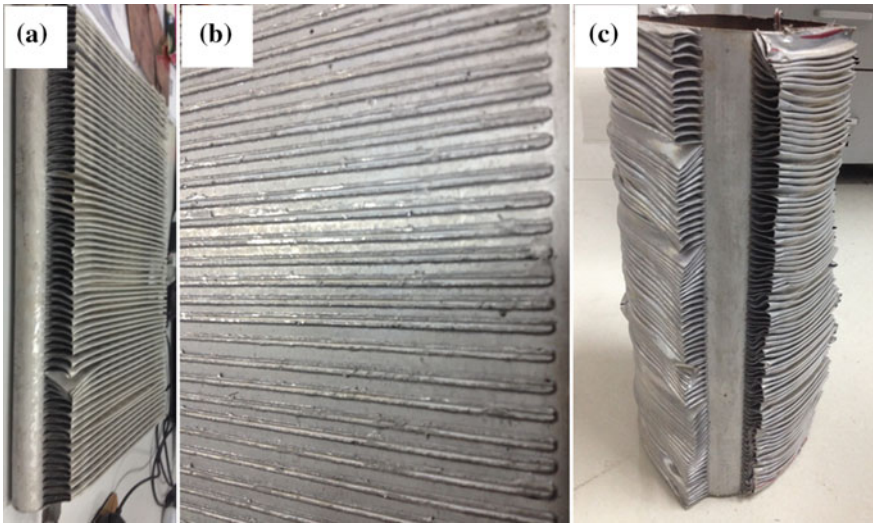

Fig. 7 Samples of air cooled island brazed by aluminum clad steel plate with the Al alloy fins. **a** the profile picture; **b** the interface between clad steel plate with the Al alloy fins; **c** the blasting samples of air cooled island

Figure 7 shows the air cooled island brazed by aluminum clad steel plate with the Al alloy fins. Obviously, the perfect interfacial bonding is presented at the base clad plate and fins as shown in Fig. 7a, b. Meanwhile, there is no interfacial delamination phenomenon between the clad plate and Al alloy fines of the blasted air cooled island as shown in Fig. 7c. Therefore, the aluminum clad steel plates can be used in the power station.

Summaries

(1) Through cold rolling and annealing heat treatment process, the aluminum clad steel plates with the 50–70 μm aluminum cladding layer have been successfully fabricated to used as heat sink substrate in the air cooling island;
(2) The tensile properties of aluminum clad steel plates reveal a slight anisotropy, which is attributed to the unique elongated grains of steel substrate, the clad plates exhibit a superior tensile elongation and slight interfacial delamination, and highest value of multiple bending fracture times is located at the clad plate along the angle of 45°;
(3) The brazing interfacial quality of aluminum clad steel plate and Al alloy fins is perfect, there is no interfacial delamination phenomenon.

Acknowledgements This work is financially supported by the National Natural Science Foundation of China (NSFC) under Grant No. 51601055, 51304059, the Hebei Science and Technology program under Grant No. 130000048, the National Natural Science Foundation of Hebei Province under Grant Nos. E201620218 and QN2016029.

References

1. H. Kawase, M. Makimoto, K. Takagi, Y. Ishida, T. Tanaka, Development of aluminum clad steel by roll bonding. Trans. ISIJ **23**, 628–632 (1983)
2. M.M. Atabaki, M. Nikodinovski, P. Chenier, J. Ma, M. Harooni, R. Kovacevic, Welding of aluminum alloys to steels: an overview. J. Manuf. Sci. Prod. **14**, 59–78 (2014)
3. L. Li, K. Nagai, F.X. Yin, Progress in cold roll bonding of metals. Sci. Technol. Adv. Mater. **9**, 1–11 (2008)
4. Y. Wang, S.G. Zhou, K.S. Vecchio, Annealing effects on the microstructure and properties of an Fe-based metallic-intermetallic laminate (MIL) composite. Mater. Sci. Eng., A **665**, 47–58 (2016)
5. Y. Wang, K.S. Vecchio, Microstructure evolution in a martensitic 430 stainless steel-Al metallic-intermetallic laminate (MIL) composite. Mater. Sci. Eng., A **643**, 72–85 (2015)
6. Y. Wang, K.S. Vecchio, Microstrcutre evolution in Fe-based-aluminide metallic-intermetallic laminate (MIL) composites. Mater. Sci. Eng., A **649**, 325–337 (2016)
7. P.C. Tortorici, M.A. Dayananda, Phase formation and interdiffusion in Al-clad 430 stainless steels. Mater. Sci. Eng., A **244**, 207–215 (1998)
8. H.D. Manesh, A.K. Taheri, The effect of annealing treatment on mechanical properties of aluminum clad steel sheet. Mater. Des. **24**, 617–622 (2003)
9. W.S. Hwang, T.I. Wu, W.C. Sung, Effect of heat treatment on mechanical property and microstructure of aluminum/stainless steel bimetal plate. J. Eng. Mater. Technol. **134**, 014501-1-6 (2012)
10. A. Nishimoto, K. Akamatsu, Preparation of homogeneous Fe-Al intermetallic compound sheet by multi-layered rolling and subsequent heat treatment. Mater. Sci. Forum **561–565**, 857–860 (2007)
11. H.Y Wu, S. Lee, J. Wang, Solid-state bonding of iron-based alloys, steel–brass, and aluminum alloys. J. Mater. Process. Technol. **75**, 173–179 (1998)
12. M. Talebian, M. Alizadeh, Manufacturing Al/steel multilayered composite by accumulative roll bonding and the effects of subsequent annealing on the microstructural and mechanical characteristics. Mater. Sci. Eng., A **590**, 186–193 (2014)
13. M. Soltan, A. Nezhad, A. Haerian Ardakani, A study of joint quality of aluminum and low carbon steel strips by warm rolling. Mater. Des. **30**, 1103–1109 (2009)
14. X. Liu, S. Lan, J. Ni, Analysis of process parameters effects on friction stir welding of dissimilar aluminum alloy to advanced high strength steel. Mater. Des. **59**, 50–62 (2014)
15. K. Kimapong, T. Watanabe, Lap joint of A5083 aluminum alloy and SS400 steel by friction stir welding. Mater. Trans. **46**, 835–841 (2005)
16. K. Lee, S. Kumai, T. Arai, Interfacial microstructure and strength of steel to aluminum alloy lap joints welded by a defocused laser beam. Mater. Trans. **46**, 1847–1856 (2005)
17. R.F. Qiu, H.X. Shi, K. Zhang, Y. Tu, C. Iwamoto, S. Satonaka, Interfacial characterization of joint between mild steel and aluminum alloy welded by resistance spot welding. Mater. Charact. **61**, 684–688 (2010)
18. M. Acarer, B. Demir, An investigation of mechanical and metallurgical properties of explosive welded aluminum-dual phase steel. Mater. Lett. **62**, 4158–4160 (2008)
19. S.H. Choi, J.W. Kwon, K.H. Oh, Prediction of inhomogeneous texture in clad sheet metals by hot roll bond method. Met. Mater. **2**, 133–140 (1996)

20. S.C. Pan, M.N. Huang, G.-Y. Tzou, S.W. Syu, Analysis of asymmetrical cold and hot bond rolling of unbounded clad sheet under constant shear friction. J. Mater. Process. Technol. **177**, 114–120 (2006)
21. Y. Jiang, D.S. Peng, D. Lu, L.X. Li, Analysis of clad sheet bonding by cold rolling. J. Mater. Process. Technol. **105**, 32–37 (2000)
22. H.R. Akramifard, H. Mirzadeh, M.H. Parsa, Cladding of aluminum on AISI 30 4L stainless steel by cold roll bonding: mechanism, microstructure, and mechanical properties. Mater. Sci. Eng., A **613**, 232–239 (2014)
23. H.D. Manesh, A.K. Taheri, Study of mechanisms of cold roll welding of aluminum alloy to steel strip. Mater. Sci. Technol. **20**, 1064–1068 (2004)
24. G. Tzou, M. Huang, Analytical modified model of the cold bond rolling of unbounded double-layers sheet considering hybrid friction. J. Mater. Process. Technol. **140**, 622–627 (2003)
25. M. Voncina, H.S. Hrenko, J. Medved, Interaction between Al99.5 and stainless steel at elevated temperature and pressure. RMZ—M&G **62**, 213–224 (2015)
26. R. Jamaati, M.R. Toroghinejad, Cold roll bonding bond strengths: review. Mater. Sci. Technol. **27**, 1101–1108 (2011)
27. S.H. Choi, K.H. Kim, K.H. Oh, D.N. Lee, Tensile deformation behavior of stainless steel clad aluminum bilayer sheet. Mater. Sci. Eng., A **222**, 158–165 (1997)
28. Q. Qin, Z.H. Wu, Y. Zang, B. Guan, F.X. Zhang, Warping deformation of 316l/q345r stainless composite plate after removal strake. World J. Eng. **13**, 206–209 (2016)
29. Q. Qin, Z.H. Wu, Y. Zang, B. Guan, A simulation study on the multi-pass rolling bond of 316L/Q345R stainless clad plate. Adv. Mech. Eng. **7**, 1–13 (2015)
30. D.N. Lee, Y.K. Kim, Tensile properties of stainless steel-clad aluminum sandwich sheet metals. J. Mater. Sci. **23**, 1436–1442 (1988)
31. H.Y. Wang, X. Li, Z.H. Wang, D.W. Zhao, D.H. Zhang, Analysis of sandwich rolling with two different thicknesses outer layers based on slab method. Int. J. Mech. Sci. **106**, 194–208 (2016)
32. P.S. Stieif, Interfacial instabilities in an unbonded layered solid. Int. J. Solids Struct. **26**, 915–935 (1990)
33. S.L. Semiatin, H.R. Piehler, Forming limits of sandwich sheet materials. Metall. Trans. A **10**, 1107–1118 (1979)
34. F. Afrouz, A. Parvizi, An analytical model of asymmetric rolling of unbounded clad sheets with shear effects. J. Manuf. Process. **20**, 162–171 (2015)
35. R. Uscinowicz, Experimental identification of yield surface of Al-Cu bimetallic sheet. Compos. B **55**, 96–108 (2013)
36. Y. Kimura, T. Inoue, F.X. Yin, K. Tsuzaki, Inverse temperature dependence of toughness in an ultrafine grain-structure steel. Science **320**, 1057–1059 (2008)
37. S.M. Allen, E.L. Thomas, *The Structure of Material* (Wiley, 1999), pp. 359–363
38. L.J. Huang, L. Geng, *Discontinuously Reinforced Titanium Matrix Composites* (Springer, 2007), pp. 1–180
39. A. Cetin, C. Bernardi, A. Mortensen, An analysis of the tensile elongation to failure of laminated metal composites in the presence of strain-rate hardening. Acta Mater. **60**, 2265–2276 (2012)